6th International Conference on Advances in Experimental Structural Engineering
11th International Workshop on Advanced Smart Materials and Smart Structures Technology
August 1-2, 2015, University of Illinois, Urbana-Champaign, United States

Pounding-Induced Stress Wave Analysis and Mitigation of Highway Bridges Under Earthquakes

Suchao Li[1*], Anxin Guo[2], Lili Cui[3], Chenxi Mao[4] and Hui Li[5]

1 *Assistant Professor, Ministry of Education Key Laboratory of Structural Dynamic Behavior and Control, School of Civil Engineering, Harbin Institute of Technology, Harbin 150090, China.*
E-mail: lisuchao@hit.edu.cn
2 *Professor, Ministry of Education Key Laboratory of Structural Dynamic Behavior and Control, School of Civil Engineering, Harbin Institute of Technology, Harbin 150090, China.*
E-mail: guoanxin@hit.edu.cn
3 *Ph.D,, School of Civil Engineering, Harbin Institute of Technology, Harbin 150090, China.*
E-mail: cuililihit@126.com
4 *Researcher, Institute of Engineering Mechanics, China Earthquake Administration, Harbin, 150090, China.*
E-mail: maochenxi@iem.ac.cn
5 *Professor, Ministry of Education Key Laboratory of Structural Dynamic Behavior and Control, School of Civil Engineering, Harbin Institute of Technology, Harbin 150090, China.*
E-mail: lihui@hit.edu.cn

ABSTRACT
Seismic colliding between adjacent structures without enough distance may lead to considerable structural damage or even collapse during large earthquakes. Additionally, during the contact-separation process, pounding-induced waves not only increase internal damage of the structure but also have significant effect on the acceleration measurement. To investigate the propagation behavior of the colliding-induced stress wave and the pounding mitigation effects of shape memory alloy pseudo-rubber shock absorber devices (SMAPR-SADs) on adjacent superstructures, a series of shaking table tests on a 1:30 scaled steel highway bridge model are performed. Then, the effect of stress waves on the acceleration signals of bridge structures is firstly investigated. The characteristics of pounding stress waves are analyzed based on wave theory, the cross wavelet transform and wavelet coherence analysis. The amplitude and absolute energy of the stress waves are compared between the original structure and after the installation of SMAPR-SADs. Furthermore, the mitigation mechanism of SMAPR-SADs on pounding-induced stress waves is interpreted. Results show that SMAPR-SAD has stable energy absorption ability and could obviously reduce the amplitude and energy of the pounding stress waves, and also lower the corresponding effect on the accuracy of the measurement system.

KEYWORDS: *pounding stress wave, characteristics analysis, mitigation strategy, SMAPR-SADs, bridge pounding*

1. INSTRUCTION

Structural pounding between adjacent structures such as insufficiently separated buildings and bridge decks frequently occurred during severe earthquakes. Filed observations and analytical studies on pounding mechanism and disaster show that pounding is often the primary cause for the damage of superstructure and initiation of collapse [1, 2, 3]. Pounding between adjacent structures will suddenly change the momentum of the system and often generate acceleration impulse and stress waves. The stress wave propagation in the structures does not only lead to the structural damage, but also affect the accuracy of data acquisition system during the lab test or field site measurement. Generally, the damage induced by impact stress wave can be attributed to the following aspects: (1) the incident compression wave, (2) the tensile wave originated from the input compression wave through the reflection on a free surface, and (3) their interaction or combination. The former one usually could directly leads to structural damage or collapse due to the large intensity, and the latter two often results in crack, scabbing or even dynamic fracture to the materials like rock and concrete [4]. The tensile wave will also extend the crack width or increase the structural damage [5].

On the other hand, the stress waves also have an influence on the accuracy of the measurement system, especially for the acceleration signals during the impact tests. In 1992, the effect of stress wave on acceleration sensor was measured in Caltrans I-10/215 interchange bridge during Landers earthquake in Southern California [6]. Researchers found that the acceleration spikes did not occurred at the same time for the accelerometers in

different locations, and the reason is finally attributed to the pounding wave stress propagation. Similar phenomenon is also found in the acceleration signals of superstructure response during base-isolated buildings pounding against moat wall [7]. In fact, the obtained data from the accelerometer is a combination of global vibration and local vibration, and the local vibration information could not represent the total response of the system, and vice versa. So if the effect of stress waves on the test signals is not considered and distinguished, the estimation of structural response will be inaccurate or even wrong. Unfortunately, studies focusing on this effect and corresponding mechanism is few, and much further work needs to be done. Additionally, in order to weaken the stress wave reflection effect during the concrete-to-concrete impact test, a buffer was used to partially fix one end of the specimen [8]. Nevertheless, the mitigation of pounding stress waves for the infrastructures are seldom considered and reported in the past researches. Therefore, it is necessary to develop high-performance energy absorbing devices with both of residual deformation self-recovery ability and stress wave absorption ability.

This paper first presents an experimental study on shape memory alloy pseudo-rubber shock absorber devices (SMAPR-SADs). Shaking table test of a scaled-bridge is then conducted and both of the global vibration signals and the local vibration signals are collected. Based on the experimental results, the characteristics of pounding stress wave are analyzed according to wave theory, and the control effect of SMAPR-SADs on pounding mitigation of highway bridges is also investigated. Subsequently, the mechanism of pounding mitigation of SMAPR-SADs is analyzed through the energy dissipation ability and stress wave absorption theory.

2. BEHAVIOR OF SMAPR-SADS UNDER CYCLIC LOADING

Shape memory alloy pseudo-rubber (SMAPR) is a kind of porous material with internal dry friction. It is made by thin SMA wires (0.1-0.5mm in diameter) through wrapping, weaving, rolling, stamping and heat treatment process. The mechanical properties of SMAPR present a strain hardening feature which can prevent shock absorber devices (SADs) from sustaining too large deformation. At the same time, it also has good corrosion resistance and large damping capacity resulting from internal dry friction, which are superior to rubber. Additionally, SMAPR has excellent self-recovery ability and good repeatable behavior after residual deformation recovered [9]. When SMAPR is heated over the austenitic start temperature, the residual deformation due to large excitations will disappear gradually. In this study, the SMAPR-SADs specimens were made by martensite NiTi (50 at.% Ni) SMA wires with a diameter of 0.2mm. The SMAPR-SADs are shown in Figure 2.1.

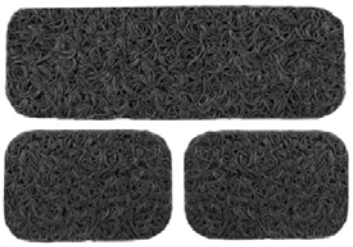

Figure 2.1 Shape memory alloy pseudo-rubber shock absorber

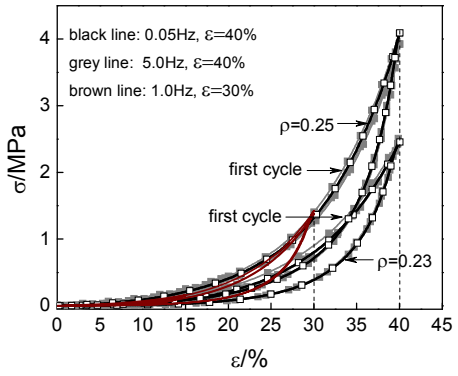

Figure 2.2 Stress-strain curves of SMAPR-SADs under different loading frequencies

The mechanical test of SMAPR-SADs were carried out on an Instron 8801 test machine at the Mechanics Test Centre at Harbin Engineering University. Considering that bridge pounding is an impact process, it is necessary to investigate the loading rate effect on the behavior of SMAPR-SADs. Therefore, four loading frequencies, 0.05, 1.0, 3.0 and 5.0 Hz, were adopted during the tests, and ten cycles were repeated for each loading case. During the cyclic compression test, the maximum loading velocity is 0.39m/s which is close to the maximum relative velocity of the adjacent decks during the shaking table test in this study. Figure 2.2 shows the stress-strain relationship of SMAPR-SADs with different nominal densities under loading frequencies of 0.05, 1.0 and 5.0 Hz, respectively. It is clearly seen that SMAPR-SADs are rate independent and the stress-strain curves overlaps very well under different frequencies after the second cycles.

3. POUNDING MITIGATION TEST OF HIGHWAY BRIDGE

3.1 Scaled highway bridge model

To verify the pounding mitigation effect of SMAPR-SADs, a highway bridge model with two segments is designed and manufactured. The setup of the highway bridge model is shown in Figure 3.1. The bridge model is approximately designed based on a standard prototype structure with a length scaling of 1:30, and the corresponding scaled gap size is 2.5 mm. Each deck of the steel bridge model has a rectangular shape with 1000 mm×400 mm in plane and 20 mm in thickness with total mass of 63.8kg. The two decks are supported on three frames with six columns. All of the columns have the identical rectangular cross section of 60 mm×16mm. In this study, four stainless steel rulers are used as leaf springs with cross section of 20mm×1.2mm to represent the bearings, and both ends of the ruler are clamped with fixtures, which are mounted on the steel plates at the top of columns. To adjust the fundamental frequencies of the adjacent decks and ensure the occurrence of pounding, the effective bending length of the rulers in the two spans is set as 4×60mm and 4×100mm, respectively. Two oil containers filled with silicone oil are used for the dampers to adjust the damping of the structure. During the pounding mitigation test cases, the SMAPR-SADs are installed at the expansion joint by using a very thin glue (see Figure 3.2).

Figure 3.1 1:30 scaled highway bridge model

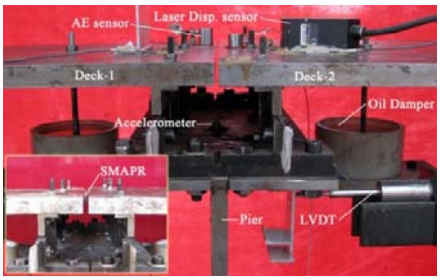

Figure 3.2 Bridge with/without control

3.2 Equipment and shaking table test scheme

For the highway bridge model, the global vibration signals such as acceleration and displacement are all measured during the test. Additionally, the local vibration signals like pounding stress waves are also collected. The measurement system of the bridge model is shown in Figure 3.3. Totally six B&K 4507B accelerometers, three LVDTs, three LK-G150 laser displacement transducers are used for testing the responses of the bridge model, and the data sampling rate is 10k Hz so as to capture the acceleration more accurately. The R15α acoustic emission sensors (AE-1~AE-7), made by MISTRAS Group, Inc., are installed on the typical location of bridge model such as the expansion joint, and both ends of decks and piers. The aim of using AE sensors here is to obtain more pounding stress wave information during the instantaneous colliding. The sample frequency and the trigger threshold of the AE system are set as 2.0MHz and 40.0 dB, respectively.

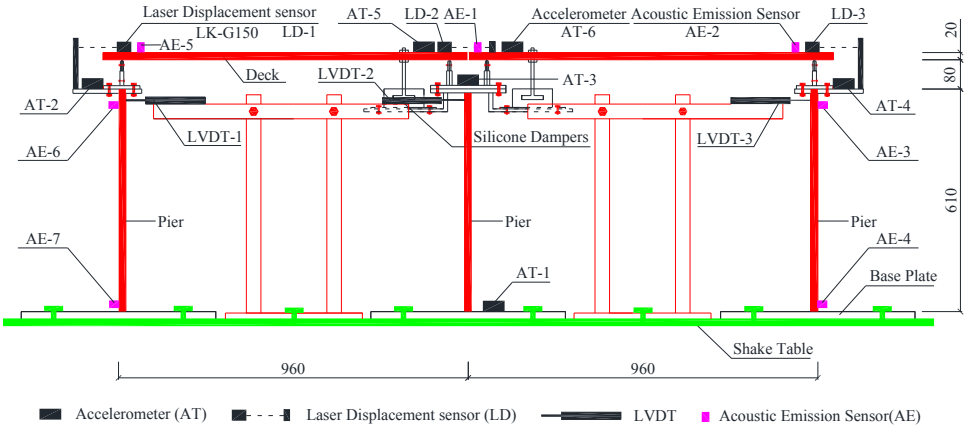

Figure 3.3 Instrumentation and measurement system of shaking table test

The data acquisition system includes a NI PXI-8108 controller, a NI PXI-4462 (24Bit) dynamic signal analyzer and a NI PXI-6123S series multifunction DAQ device. The LabVIEW software [10] is used for the data recording and visualization.

The experiments are then performed on a uniaxial seismic shaking table with size of 3m×4m at Harbin Institute of Technology. The facility is capable of producing a maximum horizontal acceleration of ±1.5g at the maximum preload of 12 tons, and the working frequency ranges from 0 to 25 Hz. The maximum velocity and displacement can be up to ±0.76m/s and ±0.125m, respectively.

4. EXPERIMENTAL OBSERVATIONS AND RESULTS ANALYSIS

4.1 Pounding stress waves measurement and characteristics analysis in the highway bridges

In this study, the acceleration sensors were also affected by the pounding stress wave. As shown in Figure 4.1, a large minus acceleration spikes occurred during the pounding separation process, which could not been easily explained according to the existing colliding theory and contact element models.

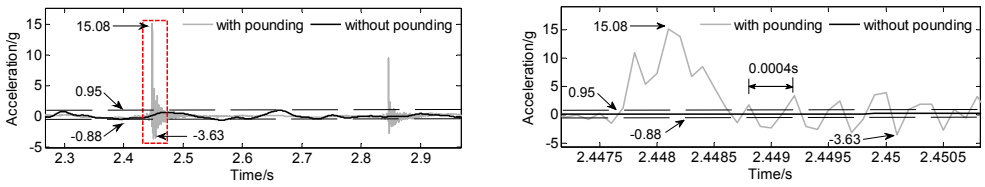

(a) Acceleration response of bridge pounding (b) One acceleration spikes enlargement

Figure 4.1 Effect of pounding stress waves on the acceleration signals under El Centro earthquake

To investigate the reason of above phenomenon, the collected signals of AE sensors during the colliding process were analyzed. Totally two acoustic emission sensors distribution schemes is conducted during the test. The first distribution scheme is shown in Figure 3.3, and the other scheme is given in Figure 4.2.

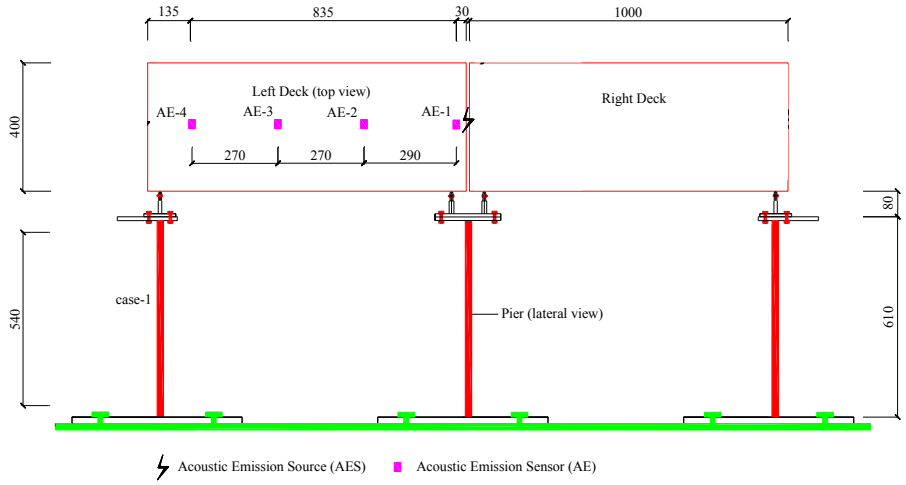

Figure 4.2 Acoustic emission sensors distribution during the test

Figure 4.3 shows the pounding stress wave propagation during the bridge decks under the AE sensor distribution in Figure 4.2. It is clearly found that the stress wave triggered the AE sensors from AE-1 to AE-4 one after one. According to the one-dimensional wave theory, the compression wave propagation velocity in the homogeneous material can be estimated by $c_0 = \sqrt{E / \rho_m}$, where E and ρ_m is the elastic modulus and density of the material, respectively. For steel material, the elastic modulus is 2.05×10^5 MPa and the density is 7800kg/m^3, then, the compression wave velocity is calculated to be 5126m/s. The average velocity of the stress wave calculated from

Figure 4.3 is about 5120m/s, which is close to the theoretical stress wave velocity in steel material. Therefore, the pounding stress waves in bridge decks is mainly recognized as compressional wave.

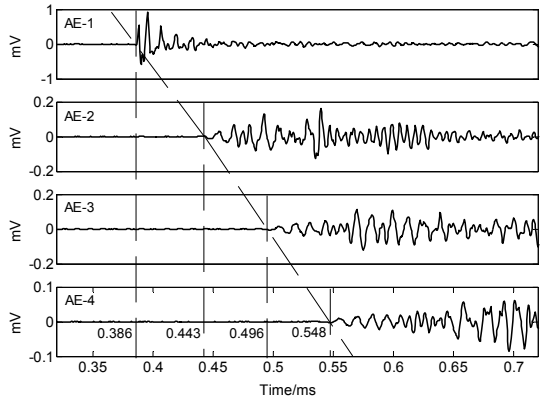

Figure 4.3 Pounding stress wave propagation during the bridge decks

For another AE sensors distribution scheme in Figure 3.3, the test results were given in Table 4.1. It is found that the velocities of stress wave in bridge decks during different poundings are relatively close, with an average velocity about 5020m/s, which also indicates the stress waves in bridge decks is compressional wave. However, according to the signals of AE-3 and AE-4 sensors distributed in bridge piers, the difference of stress wave velocity propagated in it is much larger (864m/s). The corresponding wave propagation velocity in piers is also lower than that of bridge decks.

Table 4.1 Measurement of velocity of pounding stress waves

Sensor number	AE-1 & AE-2	AE-2 & AE-3	AE-3 & AE-4
Distance between AE sensors (m)	0.835	-	0.540
Time difference during 1st pounding (μs)	172	154	176
Wave velocity during 1st pounding (m/s)	4854	-	3068
Time difference during 2nd pounding (μs)	161	166	235
Wave velocity during 2nd pounding (m/s)	5186	-	2204

To investigate the characteristics of the stress waves in the piers, the wave theory for Bernoulli-Euler beams were adopt [11]. The approximate velocity of bending wave in circular rod can be calculated by $c = \sqrt{2\pi f c_0 r_g}$, where f is the frequency of bending wave, $c_0 = \sqrt{E/\rho_m}$ and $r_g = \sqrt{I/A}$. Therefore, the velocity of bending wave is dependent on the frequency of bending waves. For example, the dominant frequency of the signal in AE-3 and AE-4 during the first pounding in Table 4.1 are 76.7 kHz. Based on the approximate estimation equation of bending wave velocity, the theoretical wave propagation velocity is 3390m/s, which is close to the experimental results. Combined with the boundary condition and the impact source of the pier, it is deduced that the stress waves in piers are bending waves.

From above analysis, it is clear that the pounding stress wave exists in bridge decks during colliding. It is helpful to explain the minus spikes in the acceleration history signals after pounding. It is also helpful to understand the time difference of the peak accelerations for different located accelerometers in former studies.

4.2 Pounding mitigation effect on stress waves

This section mainly investigated the control effect of SMAPR-SADs on the pounding stress waves during earthquakes. To better understand the characteristics and corresponding control effect of the stress wave signals in the bridge model, the time-frequency transform based on continuous wavelet transform method was conducted to analyze the amplitude and energy distribution of stress waves during the colliding. The results of the time-frequency transform to the stress wave signals in the bridge decks under El Centro earthquake records (PGA=400gal) were shown in Figure 4.4.

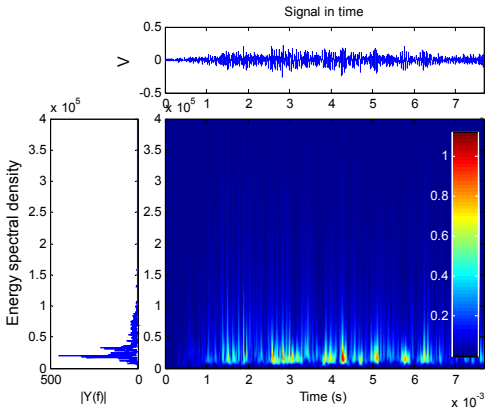

(a) AE-1 (without SMAPR-SADs)

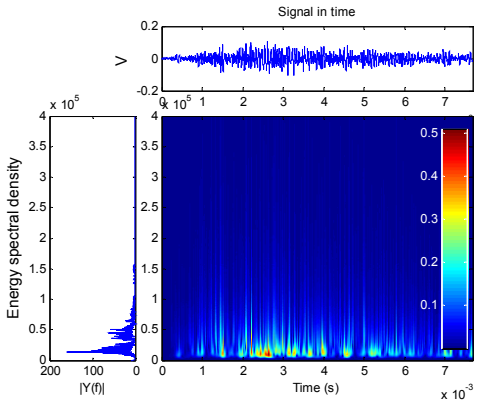

(b) AE-2 (without SMAPR-SADs)

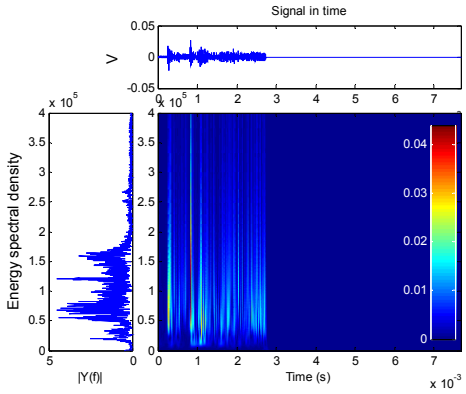

(c) AE-1 (with SMAPR-SADs)

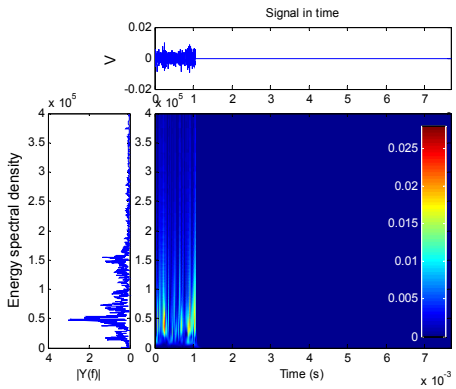

(d) AE-2 (with SMAPR-SADs)

Figure 4.4 Pounding stress wave signals and time-frequency analysis with and without SMAPR-SADs

First of all, it is found that all the AE sensors (AE-1 to AE-4) could detect the stress wave signals under the non-control cases. However, only the AE sensors (AE-1 and AE-2) on the bridge decks could detect the stress waves after installation of SMAPR-SADs, and the AE sensors (AE-3 and 4) on the piers were not even triggered by the stress waves due to its too small intensity. From stress wave signal histories in Figure 4.4 (a) and (b), the amplitude of the signals from AE-1 to AE-2 decreases about 50% for non-controlled cases. Similar results are also found for the controlled cases in Figure 4.4 (c) and (d), which represents the energy dissipated by the constant material damping. Compared with Figure 4.4 (a) and Figure 4.4 (c), the amplitude of the stress wave signals decreased as much as 96% in control and non-control cases. However, this reduction of amplitudes results from the internal friction effect.

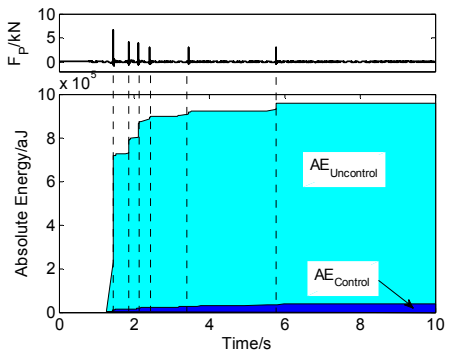

a) El Centro record

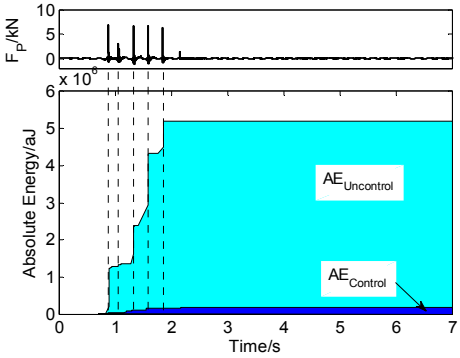

b) Kobe record

Figure 4.5. Absolute energy of pounding waves versus time during El Centro and Kobe records

Generally, the energy envelope is usually taken as an important evaluation parameter of a signal, and it also can represent the signal magnitude and scale. Therefore, the absolute energy versus time for El Centro and Kobe earthquake records (PGA=400gal) in both of control and non-control cases were shown in Figure 4.5. To verify the validity of the measured stress waves during the colliding, the pounding force history were also given in this figure. It is noted that the energy curves increases suddenly at the same time of pounding occurrence, and a good consistency was found between the above two histories. Figure 4.5 also shows that the stress wave energy of the controlled bridge decreased more than 90% compared to the non-controlled system. So it could be indicated that SAMPR-SADs could greatly reduce both of the amplitude and energy of pounding-induced stress waves, which will finally make good protection on the structures.

Furthermore, the decrease of the stress wave signals will also help to reduce the effect of stress wave signals on the measurement system. The comparison of acceleration histories of AT-6 on the right deck before and after installing the SMAPR-SADs are presented in Figure 4.6.

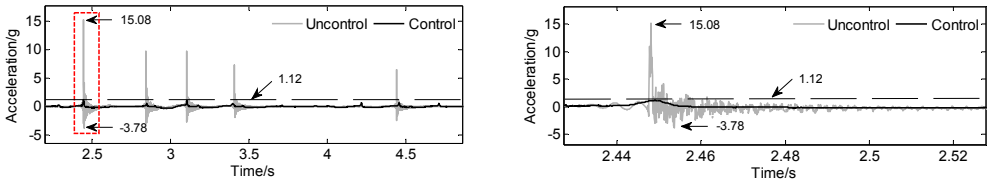

(a) Acceleration history of right deck (b) Acceleration spikes enlargement

Figure 4.6 Effect of pounding stress waves on the acceleration signals under El Centro earthquake

Due to the mitigation of the global vibration, the severe decrease of pounding force greatly reduce the magnitude of the pounding-induced stress waves, and the reflection and refraction phenomenon will also become weak. These stress waves in bridge decks will quickly disappear due to the material damping during the propagation. Therefore, the acceleration history curves of the controlled bridge model become smooth after pounding and the negative acceleration spikes also disappear.

During the stress waves propagating in SMAPR-SADs, the micro SMA spirals will generate shape deformation and local vibration due to the high stress loading. In this process, some of the impact wave energy will be stored as potential energy in the SADs and some of energy will be dissipated by the material damping of SMA. The shape change often plays an important role in the energy absorption and dissipation process. Former studies showed that the decay curves of porous material is usually described as exponential function and the corresponding decay rate is also more faster than the solid materials [12]. Additionally, during the shape change process of micro ‘open cells’, limited sliding will also occur between the micro SMA spirals. So the internal frictional force will convert the kinetic energy of incident waves into heat, and which eventually dissipates the input energy.

CONCLUSIONS

To investigate and mitigate the pounding stress waves in highway bridges, shape memory alloy pseudo-rubber shock absorber devices was presented and a series of shaking table tests were conducted. Based on the analysis presented herein, main conclusions are summarized as follows:

(1) Pounding stress waves existed in different components of highway bridges are not the same, i.e., the stress waves in bridge decks and piers are compressional wave, and bending waves, respectively. Additionally, the correlation between the stress wave propagation is also affected by the complicated boundary condition of the bridges.

(2) SMAPR-SADs can reduce local vibration of the highway bridges. Both of the amplitude and absolute energy of pounding-induced stress wave could be reduced more than 90% after installation of SMAPR-SADs.

(3) The mechanism of pounding mitigation of SMAPR-SADs comes from the decrease of coefficient of restitution and specific micro changeable lattice structure. The input energy of incident waves is finally absorbed by the large restorable deformation and dissipated by the internal friction as well as material damping.

AKCNOWLEDGEMENT

This study is financially supported by the financial supports from the National Key Technology Support Program with Grants No 2015BAK17B04, National Natural Science Foundation of China with Grant Nos 51222808 and 51308170, and China Postdoctoral Science Foundation with Grant No. 2013M541384.

REFERENCES

1. Karayannis C G, Favvata M J. (2005). Earthquake-induced interaction between adjacent reinforced concrete structures with non-equal heights. *Earthquake Engineering and Structural Dynamics*. **34:1**, 1-20.
2. Anagnostopoulos S A, Karamaneas C E. (2008). Use of collision shear walls to minimize seismic separation and to protect adjacent buildings from collapse due to earthquake-induced pounding. *Earthquake Engineering and Structural Dynamics*. **37:12**, 1371-88.
3. Abdel Raheem S E. (2006). Seismic pounding between adjacent building structures. *Journal of Structural Engineering*: 6, 66-74.
4. Fabrice G, Gilles P C. (2002). Coupled damage and plasticity modelling in transient dynamic analysis of concrete. *International Journal for Numerical and Analytical Methods in Geomechanics*. **26**, 1-24.
5. Flocker F W and Dharani L R. (1997). Modelling fracture in laminated architectural glass subject to low velocity impact. *Journal of Materials Science*. **32**, 2587-2594.
6. Malhotra P K, Moth J H, Anthong F S. (1995). Seismic interaction at separation joints of an instrumented concrete bridge. *Earthquake Engineering and Structural Dynamics*. **24:3**, 1055-1067.
7. Masroor A, Mosqueda G. (2002). Experimental simulation of base-isolated buildings pounding against moat wall and effects on superstructure response. *Earthquake Engineering and Structural Dynamics*. **41**, 2093-2109.
8. Jan G M, Arjan F P, Hans W R and Theo M. (1991). Load-time response of colliding concrete bodies. *Journal of Structural Engineering*. **117**, 354-374.
9. Li S C, Mao C X, Li H and Zhao Y G. (2011). Mechanical properties and theoretical modeling of self-centering shape memory alloy pseudo-rubber. *Smart Material and Structures*. **20:11**, 115008.
10. National Instrument Company (2013). LabVIEW Measurement Manual 2013, Austin, Texas.
11. Ya.S. Uflyand. (1948). The propagation of waves in the transverse vibration of bars and plates. *Prikladnaya Matematika I Mekhanika*.**12**: 287-300.
12. Kalliopi K A. (2006). Pore Structure of Cement-Based Materials: Testing, Interpretation and Requirements. Taylor & Francis Group, London.